A reaction matrix method in waveguides with coupling resonances

Lei Xiong, Wenping Bi, Yves Aurégan
Laboratoire d'Acoustique de l'Université du Maine,
UMR CNRS 6613
Av. O Messiaen, 72085 LE MANS Cedex 9,France

Summary

A Reaction Matrix (R-matrix) method is used to investigate wave propagation through locally perturbed acoustic waveguide. A coupling matrix is introduced to describe the coupling between the discrete modes via the semi-infinite ducts. Two cases are considered: a waveguide coupled with cavity, and with impedance wall. In both cases, Fano resonances and trapped modes are all observed at some specific geometry parameter values and particular frequencies. Matrix H_{eff} is developed to locate the positions and widths of the resonances of the open system. By varying a parameter continuously, avoided crossings of the resonances in the complex plane are always observed. Because of the interference of two neighbor resonances via the duct, the width of one of the resonances will almost vanish, resulting in the strong localization of the pressure field in the waveguide. More importantly, the R-matrix method also allows an easy treatment of the non-separable problem along transverse and axial directions. This method is also applied to a lined wall with varying impedance along the axis. The effects of the Fano resonances and trapped modes on the transmission and reflection coefficients are analyzed. By tracing the motions of the eigenvalues of the matrix H_{eff}, the Fano line-shape transmission coefficients can be well predicted at some particular frequency.

PACS no. 43.20.Mv, 43.20.Ks

1. Introduction

Resonance is a universal characteristic in many different physical systems. Many investigations have been done to use the coupling of the local resonance to get extraordinary phenomenas, for example metamaterials[1, 2, 3, 4]. Porous materials including periodic subwavelength resonators have also been proposed to try to gain an additional absorption peak below the $\lambda/4$ resonance[5]. Recently, S. Hein *et al.*[6] used the finite-element method to numerically compute the acoustic resonances in 2D acoustical duct-cavity systems. They concluded that the embedded trapped modes occur only for very particular geometry parameters and frequencies. One kind of trapped mode is due to the destructive interference between two resonant modes via a common continuum. Comparing to the work of S. Hein *et al.* and Duan[7], instead of computing the resonances of the open system directly, we developed a coupling matrix to describe the coupling between the resonances of the cavity and the environment.

Due to the interaction of the trapped modes with the incoming propagating modes, Fano resonances show up in the transmission spectrum. It was first suggested by Ugo Fano[8] for the description of autoionizing atomic states. In contrast to a Lorentzian resonance, the Fano resonance exhibits a distinctly asymmetric shape. Joe *et al.*[9] provided a novel insight into Fano resonance physics by simply using two weakly coupled harmonic oscillators, where one of them was driven by a periodic force.

In this paper, we use an efficient method, Reaction matrix method (R-matrix)[10], to study wave propagation through locally perturbed acoustic waveguide. The R-matrix method has one important advantage: it can treat easily the non-separable problem along transverse and axial directions. The R-matrix formulation was developed by Wigner and Eisenbud [10] in scattering processes in nuclear physics in the late 1940s. Recently, it was extended by Racec *et al*[11] to investigate the scattering phenomena in cylindrical nanowire heterostructures. The basic idea of this method is similar to the Multimodal method[12, 13]. For the Multimodal method, the wave function is projected in terms of a convenient transverse complete basis. However, the R-matrix method decomposes the duct into a reaction region (cavity or acoustic liner in this paper), and an asymptotic scattering region (two semi-infinite rigid leads). The wave function in the reaction region is expanded in terms of any convenient complete set of modes of *a closed cavity* with convenient boundary conditions. Using the continuity conditions of the pressure and the normal particle velocity at the interfaces between the regions, the scattering matrix is expressed in terms of the R-matrix. Using the scattering matrix, we can derive the matrix $\mathsf{H}_{\mathsf{eff}}$ of the open system, from which we can analyze the coupling of the resonances.

2. Problem formulation

In this section, we study the sound wave propagation in a two-dimensional (2D) locally perturbed waveguide of height h^*. Two configurations are considered, as illustrated in Fig.1. For configuration (A), a single cavity of depth b and length a is located in an infinite uniform duct of height h, with rigid boundary conditions on the walls. For configuration (B), it is an acoustic duct treated with a liner of length a and with a varying admitttance.

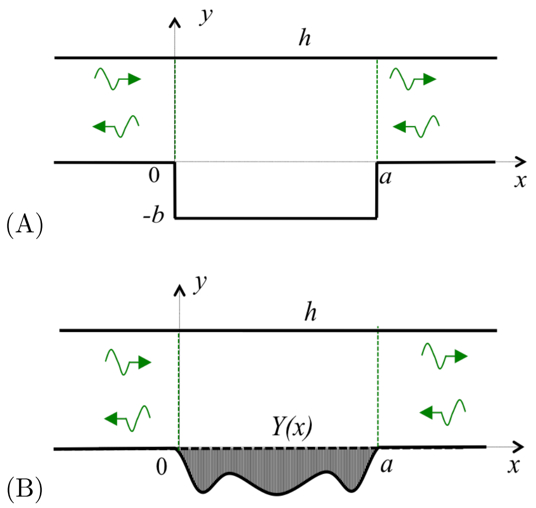

Figure 1. Two configurations are studied. (A) Acoustical duct-cavity system. (B) Acoustic duct lined with liner.

2.1. Scattering formalism

The sound pressure $p(x, y)$ satisfies the equation, Eq.(1), in the 2D-Cartesian coordinates (x, y), nondimensionalised with the duct height h^*. Here, and in the following, the asterisk marks dimensional quantities (the time dependence $e^{-j\omega^* t^*}$ will be omitted in the following).

$$\frac{\partial^2 p(x,y)}{\partial x^2} + \frac{\partial^2 p(x,y)}{\partial y^2} + K^2 p(x,y) = 0, \tag{1}$$

with $K = (\omega^*/c_0^*)h^*$ is the dimensionless frequency, c_0^* the sound speed, and ω^* the circular frequency. In the following, all quantities are non-dimensionalized: lengths with the waveguide height $h^*(h = 1$ in the following), velocities with sound speed c_0^*, densities with the ambient density ρ_0^*, and pressures with $\rho_0^* {c_0^*}^2$.

The sound pressures in different regions are piecewise solved. For the two semi-infinite uniform ducts, the pressure field is developed on a basis of duct modes. We assume that there is only one duct mode m incident from the left side of the waveguide. For the left duct $(x < 0)$, the sound pressure is written as a sum of the incident and reflected modes, and only transmitted modes for the right duct $(x > a)$:

$$p_m(x,y) = \begin{cases} e^{jK_m x}\phi_m(y) + \sum_{m'=0}^{\infty} \mathsf{R}_{m',m} e^{-jK_{m'}x}\phi_{m'}(y) \\ \sum_{m'=0}^{\infty} \mathsf{T}_{m',m} e^{jK_{m'}(x-a)}\phi_{m'}(y), \end{cases} \tag{2}$$

where $K_m^2 = K^2 - \alpha_m^2$, $\Re\{K_m\} > 0, \Im\{K_m\} > 0$, and (α_m, ϕ_m) are the eigenvalues and the eigenfunctions of the transverse eigenproblem of the uniform duct with Neumann boundary conditions.

Here, R and T are matrices linking incoming and outgoing wave components. They are also used to define the scattering matrix S, as written in Eq.(3),

$$\mathsf{S} = \begin{bmatrix} \mathsf{R} & \mathsf{t} \\ \mathsf{T} & \mathsf{r} \end{bmatrix}. \tag{3}$$

Matrices R and T (respectively, r and t) correspond to wave incident from the left (respectively, from the right).

2.2. Reaction matrix formalism

The sound pressure in the reaction region is expressed in terms of the eigenmodes $\psi_l(x, y)$ of a closed cavity of length a and width d ($d = h + b$ for (A), and $d = h$ for (B))

$$p_m(x,y) = \sum_{n=1}^{\infty} a_{mn}\psi_n(x,y). \tag{4}$$

where $\psi_n(x, y)$ satisfies the following Helmholtz equation,

$$\Delta\psi_n(x,y) + \gamma_n^2\psi_n(x,y) = 0. \tag{5}$$

The eigenvalues γ_n of a single closed rectangular cavity with rigid boundary conditions at the walls are specified by two integers (μ, ν),

$$\gamma_n = \sqrt{\left(\frac{\mu\pi}{a}\right)^2 + \left(\frac{\nu\pi}{d}\right)^2}, \tag{6}$$

where n is an integer index referring to the couple (μ,ν) of the axial and transverse indexes, with $n = 1, 2, 3, \cdots$, correspond to $(\mu,\nu) = (0,0), (0,1), (0,2), \cdots, (1,0), (1,1), (1,2), \cdots$. For the computation of configuration (B), the eigenfunctions of the closed lined cavity are projected on the basis of the eigenfunctions $\psi_n(x,y)$.

Multiplying Eq.(1) by $\psi_n(x,y)$, Eq.(5) by $p_m(x,y)$, taking the difference of the two resulting equations, integrating over $[0,a]\times[-b,h]$ ($[0,a]\times[0,h]$ for (B)), and applying the Green's theorem, with the boundary conditions of ψ_n, for configuration (A), we obtain

$$\vec{a_m}\mathsf{K_N} = \int_0^h \left\{ \frac{\partial p_m}{\partial x}\vec{\psi}\Bigg|_{x=a}^{x=0} \right\} dy, \tag{7}$$

where $\vec{a_m} = (a_{m1}, a_{m2}, a_{m3}, \cdots a_{mn}, \cdots)$, $\vec{\psi} = (\psi_1, \psi_2, \psi_3, \cdots, \psi_n, \cdots)$. And $\mathsf{K_N}$ is a diagonal matrix with elements $K_n = K^2 - \gamma_n^2$.

For the configuration (B), with normalized admittance $Y(x)$ on the wall ($y = 0, 0 < x < a$), the third kind of boundary condition has to be used, which is written as

$$\frac{\partial p(x,y)}{\partial y}\Bigg|_{y=0} = -jKY(x)\cdot p(x,0). \tag{8}$$

Then we can have

$$\vec{a_m}(\mathsf{K_N} + jK\mathsf{M}) = \int_0^h \left\{ \frac{\partial p_m^{(s)}}{\partial x}\vec{\psi}\Bigg|_{x=a}^{x=0} \right\} dy, \tag{9}$$

with

$$(\mathsf{M})_{n',n} = \int_0^a Y(x)\psi_{n'}(x,0)\psi_n(x,0)dx,$$

is the coupling matrix induced by the impedance.

To construct the scattering matrix S, the continuity conditions of the pressure and the normal velocity at the interfaces, $x = 0$ and a, are used. By Eq.(2), the first derivative along x of the pressure at the interfaces can be obtained. Substituting in the right side of the Eqs.(7)(9), writing them in a matrix form, results in

$$\mathsf{AD} = j(\mathsf{I} - \mathsf{S^T})\mathsf{K_M}\ \mathsf{R_1}. \tag{10}$$

where A is a $2M \times N$ matrix, the first M rows correspond to the wave incident from the left side, and the remainings from the right side. M is the truncated number of the transverse modes in the ducts, and N is the truncated number of the eigenmodes ψ_n. $\mathsf{D} = \mathsf{K_N}$ for (A), and $\mathsf{D} = \mathsf{K_N} + jK\mathsf{M}$ for (B). I refers to the identity matrix. 'T' indicates the transposition. $\mathsf{K_M}$ a diagonal matrix with elements K_m, and $\mathsf{R_1}$ is a $2M \times N$ matrix, in which the elements are

$$\mathsf{R_1} = \begin{pmatrix} \int_0^h \phi_1(y')\psi_1(0,y')\,dy' \\ \vdots \\ \int_0^h \phi_M(y')\psi_N(0,y')\,dy' \\ \int_0^h \phi_1(y')\psi_1(a,y')\,dy' \\ \vdots \\ \int_0^h \phi_M(y')\psi_N(a,y')\,dy' \end{pmatrix}. \tag{11}$$

By the continuity condition of the pressure at the interfaces $x = 0, a$, we have

$$\mathsf{S^T} = \left\{ \mathsf{I} - 2\left[\mathsf{I} + j\mathsf{K_M}\mathsf{R}\right]^{-1} \right\}, \tag{12}$$

where $\mathsf{R} = \mathsf{R_1}\mathsf{D}^{-1}\mathsf{R_1^T}$. Matrix $\mathsf{R_1}$ describe the coupling between the discrete modes of the closed cavity and the transverse modes of the ducts.

2.3. Matrix $\mathsf{H_{eff}}$

After embedding the system into the ducts, the discrete modes of the closed system turn over in complex resonances. A non-Hermitian effective Hamiltonian[14] operator $\mathsf{H_{eff}}$ is derived here to compute the resonances of the open system. To do that, the relation between the eigenvalues of $\mathsf{H_{eff}}$ and the poles of S matrix is first constructed. By Eq.(12) and Eq.(A14) in [14], the scattering matrix of the open cavity is rewritten as

$$\mathsf{S} = -\mathsf{I} + 2j\mathsf{R_1}\frac{1}{K^2\mathsf{I} - \mathsf{H_{eff}}}\mathsf{R_1^T}\mathsf{K_M}, \tag{13}$$

where

$$\mathsf{H_{eff}} = \mathsf{H_{in}} - j\mathsf{R_1^T}\mathsf{K_M}\mathsf{R_1} \tag{14}$$

describes the system embedded into the waveguide. $\mathsf{H_{in}}$ is the matrix for the closed cavity. For (A), it's a diagonal matrix with elements γ_n^2. For (B), it contains additional internal coupling effects, $jK\mathsf{M}$, from the admittance.

The eigenvalues K_λ^2 and eigenfunctions Ψ of $\mathsf{H_{eff}}$ are obtained by solving the following equation

$$\mathsf{H_{eff}}\Psi = K_\lambda^2\Psi. \tag{15}$$

From Eq.(13), the poles of the S matrix are determined by the eigenvalues K_λ^2 of $\mathsf{H_{eff}}$ after solving the fixed-point equations Eq.(16). The eigenvalues K_λ^2 provide not only the frequencies K_R of the resonances but also their widths Γ_R,

$$\begin{aligned} K_R &= \mathrm{Re}\{K_\lambda\}_{K=K_R}, \\ \Gamma_R &= 2\cdot|\mathrm{Im}\{K_\lambda\}|_{K=K_R}. \end{aligned} \tag{16}$$

3. RESULTS

For the sake of simplicity, the incident frequency is chosen under the first cut-off frequency in the ducts, i.e. $0 < K < \pi/h$.

3.1. Acoustical duct-cavity system

The acoustical duct-cavity system, as shown in configuration (A), is considered first. Before we discuss the numerical solutions of the open cavity, we review the corresponding closed cavity with vanishing normal velocity conditions towards the interfaces. The eigenvalues of the closed cavity with rigid boundary conditions can be computed analytically. For this closed cavity, the eigenvalues γ_n of some modes get cross when the length a is varied, i.e. the eigenvalues are equal. For example, for the modes $(\mu, \nu) = (0, 1)$ and $(2, 0)$, Eq.(6) yields the crossing point $a/h = 4$ and $b/h = 1$. However once the closed system is opened by attaching to the ducts, the resonances of the open system are generally complex valued. Matrix $\mathsf{H}_{\mathsf{eff}}$ is used to describe the coupling of the modes of the closed system via the ducts.

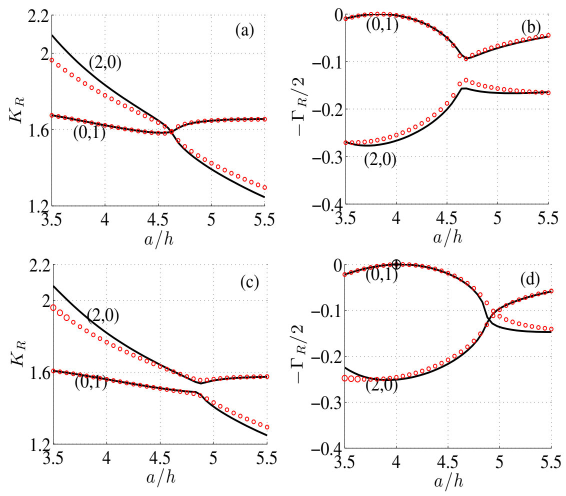

Figure 2. (Color online) Solid line: real part (a)(c) and imaginary part (b)(d) of the resonances $(0, 1)$ and $(2, 0)$ as a function of length a/h for different values of b/h by solving fixed-point equation, (a)(b)$b/h = 0.95$ and (c)(d) $b/h = 1.05$. Circle: the motions of eigenvalues K_λ of $\mathsf{H}_{\mathsf{eff}}$ with $K = 1.59$.

In Fig.2, solid lines show the motions of the modes (0,1) and (2,0) as a function of a/h with different values of b/h. The motions of eigenvalues K_λ of $\mathsf{H}_{\mathsf{eff}}$ by taking $K = 1.59$ are shown by circles. Two types of avoided crossings are observed for both the resonances and K_λ. In Figs.2(a)(b), when $b/h = 0.95$, crossing for the real and avoided crossing for the imaginary parts are found. Inversely, avoided crossing for the real and crossing for the imaginary parts, when $b/h = 1.05$, are shown in Figs.2(c)(d) . The figures show that the accidental degeneracy of the closed cavity discussed previously shows avoided crossing in the open system. In Figs.2(b)(d), due to the coupling of the resonances via the ducts, the imaginary of one resonance starts to increase and approach to "0", while the other one decreases. This effect results in a trapped mode.

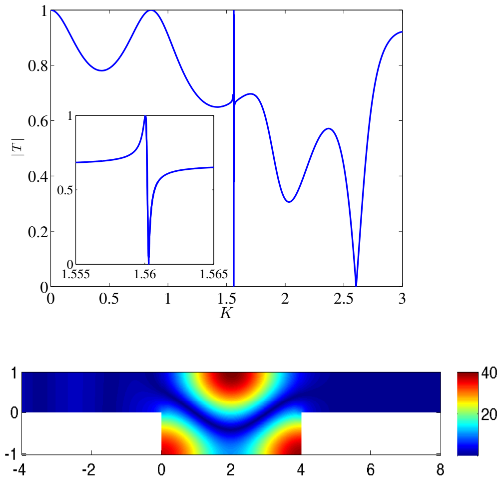

Figure 3. (Color online) Upper: Transmission coefficients as a function of frequency K with $a/h = 4$, $b/h = 1.05$. Bottom: Absolute value of the pressure field in the waveguide when $|T| = 0$.

When the trapped modes of the system are determined, we know where to look for Fano resonances. In Fig.3, the transmission coefficients $|T|$ as a function of the incident frequency K for a incoming plane mode with $a/h = 4$ and $b/h = 1.05$ are shown, where the resonance width illustrated by "$\bigoplus$" in Fig.2(d) is almost vanished. Due to the interaction of the incoming propagating duct mode and the trapped mode, the results exhibit the typical Fano resonance with antisymmetric line-shape profile (as shown in the inset) near the trapped mode frequency. The transmission coefficient $|T|$ first reaches '1' and then decreases to '0' sharply. Smaller the width of the trapped mode is, sharper and faster the coefficients change. The absolute value of the pressure field distribution in the system when the transmission is *zero* is also shown in Fig.3. We see that the pressure field in the cavity is much more higher than in the ducts, who shares the same pressure profile as the trapped mode, also shown in Fig.7(a) by Hein and Koch *et al.*[6]. The eigenfunction of the trapped mode is a strong mixing of eigenfunctions of modes (0,1) and (2,0) .

3.2. Acoustic duct lined with impedance

For configuration (B), we consider a typical acoustic liner. The impedance is written in a normalized way

$$Z(K) = Re + 1/\left[-jtan(Kd_l)\right], \tag{17}$$

where d_l is the depth of the liner, Re is the resistance. The admittance is defined by $Y(K) = 1/Z(K)$. For simplicity, uniform impedance Z without any loss, i.e. d_l is independent of the axial coordinate and $Re = 0$, is considered first. In our studies, we set $a/h = 4, M = 30, N = 30 \times 30$. When the lined cavity is closed, the eigenvalues are purely real or imaginary valued. The index to label the modes of the closed lined cavity follows the index (μ, ν) of closed rigid cavity $(0, a) \times (0, h)$ when $Y = 0$. With varying d_l, some modes get cross. However, for the open system, the resonances are complex valued. Fig.4(a) shows K_λ as a function of d_l, two types of avoided crossings for the modes who have the same parity in x-direction are observed again.

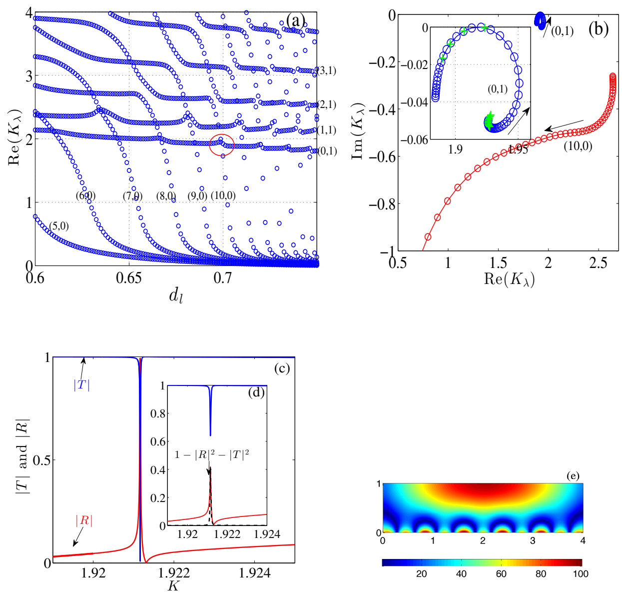

Figure 4. (Color online) Results for uniform liner with length $a = 4$. (a) Motions of Re(K_λ) as a function of d_l, with $K = 1.921$. (b) Motions of the eigenvalues of modes $(0, 1)$ and $(10, 0)$ in the complex plane. (c) Transmission and reflection coefficients as a function of K when $d_l = 0.7$. (d) Absorption is also shown by dashed line with $Re = 10^{-5}$. (e) The absolute value of pressure field distribution in the reaction region when $|T| = 0$.

The interference behaviors of the modes marked by the circle are shown in Fig.4(b). A repulsion between the two modes is observed. After the repulsion, the imaginary part of mode $(0, 1)$ approaches to "0" $d_l = 0.7$. However, the imaginary part of the other mode $(10, 0)$ moves away from the real axis. The inset in Fig.4(b) is the zoom of the mode $(0, 1)$ in the complex plane. The resonances $K_R - i\Gamma_R/2$ of the system is also shown in Fig.4(b) by '+' by solving the fixed-point equation Eq.(16). By the comparison of the two results in the inset, we can see that, by taking $K \approx K_R$, K_λ can be used to well present the resonance (0,1), as well as the condition for the trapped mode, i.e. the depth of the liner here. The effects on the wave propagation of the interference between the two resonances is illustrated by plotting the transmission and reflection coefficients in Fig.4(c), with $d_l = 0.7$. A typical Fano line shape is observed again. With the consideration of dissipation, the results are shown in Fig.4(d), an absorption (dashed line) peak is observed near the Fano resonance. The absolute value of the pressure field in the waveguide, when the transmission is zero, is shown in Fig.4(e). A strong field localization is exhibited in the lined part, it's a combination of the eigenfunctions of the two modes (10,0) and (0,1).

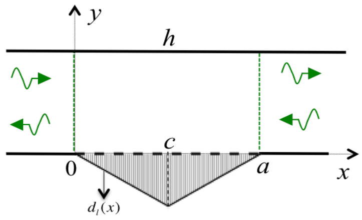

Figure 5. Schematic illustration of the non-uniform liner, the depth of the liner $d_l(x)$ is a linear function of the x-axis.

By Eq.(9) and matrix M, matrix $\mathsf{H_{eff}}$ is used to consider duct lined with non-uniform impedance. As shown in Fig.5, $x = c$ is the position of the largest depth d_{lmax}, and then the depth decreases lineally to $zero$ at $x = 0$ and $x = a$. In this paper $c = a/2$ is set. Chebyshev spectral method[15] is used to calculate the integration of matrix M. Because of the non-uniformity of the liner in the x-direction, it induces the internal coupling of the modes in the closed lined cavity, resulting in the repulsions of the real parts of the eigenvalues of $\mathsf{H_{in}}$ with varying d_{lmax}.

When the nonuniform liner is coupled to the waveguide, the $\mathsf{H_{eff}}$ is used to describe the open system. The motions of the real parts of some eigenvalues as a function of d_{lmax} are shown in Fig.6(a). Crossing and avoided crossing are observed. The same as uniform liner, some modes decrease fast with increasing d_{lmax}. However, the difference is that some of them get close to each other. It is because of the internal coupling of the modes introduced by the non-uniformity of the liner in the x-direction. When two neighbour modes of them meet with one mode $(\mu, 1)$, only one mode interferes with $(\mu, 1)$. The same as uniform liner, there are some modes decrease gradually with increasing d_l. One of them is plotted in the complex plane, see Fig.6(b). Three obvious repulsions are observed, labelled by "1,2,3" in the figure. After each repulsion, an almost vanishing width is always following. The three repulsions are corresponding to the crossings in the real parts in figure (a). Figure (c) shows the transmission and reflection coefficients when $d_{lmax} = 1.14$ is taken, which is corresponding to the " $*$ " in (b).

Fano anti-resonance and resonance is observed again. With the consideration of dissipation, the results are shown in (d), there is an absorption peak near the Fano resonance. The pressure field when the transmission is *zero* is shown in Fig.6(e).

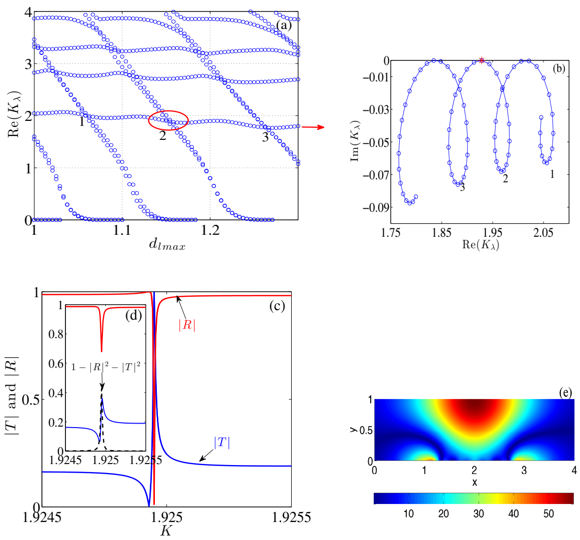

Figure 6. (Color online) Results for nonuniform liner, (a) Motions of the real part of the eigenvalues with varying d_{lmax}, with $K = 1.921$. (b) Motions of mode indicated on the left by arrow in the complex plane. (c) Transmission and reflection coefficients corresponding to the "*" in the middle figure where $d_{lmax} = 1.14$. (d) Absorption is also shown by dashed line with $Re = 10^{-5}$. (e)The absolute value of pressure field distribution in the reaction region when $|T| = 0$.

4. CONCLUSIONS

In summary, by R-matrix method, we have investigated the wave propagation in the waveguide that contains a cavity and an impedance wall. Matrix $\mathsf{H}_{\mathsf{eff}}$ is derived to analyze the couplings behaviors of the resonances. By varying a parameter continuously, avoided crossing or crossing for the real and imaginary parts are observed. Before or after the avoided crossing, one resonance can have almost vanished width, which results in the trapped modes. Due to the interference of the trapped and the incoming propagating mode, Fano antisymmetric line-shape is exhibited in the transmission spectrum. With the consideration of the dissipation in the liner, absorption peak is found near the Fano resonances.

Acknowledgement

This work has been funded by the European Union through ITN-project FlowAirS (Contract No. FP7-PEOPLE-2011-ITN-289352).

References

[1] Z. Liu, X. Zhang, Y. Mao, Y. Y. Zhu, Z. Yang, C. T. Chan, and P. Sheng: Locally Resonant sonic materials. Science 289 (2000) 1734 .

[2] Z. Liu, C. T. Chan, and P. Sheng: Analytic model of phononic crystals with local resonances. Phys. Rev. B 71 (2005) 014103 .

[3] J. Li and C. T. Chan: Double-negative acoustic metamaterial. Phys. Rev. E 70 (2004) 055602(R) .

[4] N. Fang, D. Xi, J. Xu, M. Ambati, W. Srituravanich, C. Sun, and X. Zhang: Ultrasonic metamaterials with negative modulus. Nat. Mater. 5 (2006) 452 .

[5] J-P Groby, A. Duclos, O. Dazel, L. Boeckx, et L. Kelders: Enhancing absorption coefficient of a backed rigid frame porous layer by embedding circular periodic inclusions. J. Acoust. Soc. Am.,130 (2011) 3771-3780 .

[6] S. Hein, W. Koch, and L. Nannen: Trapped modes and fano resonances in two- dimensional acoustical duct-cavity systems. Journal of Fluid Mechanics 692 (2012) 257-287 .

[7] Y. Duan, W. Koch, C. M. Linton, and M. McIVER: Complex resonances and trapped modes in ducted domains. Journal of Fluid Mechanics 571 (2007) 119.

[8] U. Fano: Effects of configuration interaction on intensities and phase shifts. Physical Review 124 (1961) 1866-1878.

[9] Yong S Joe, Arkady M Satanin and Chang Sub Kim: Classical analogy of Fano resonances. Phys. Scr. 74 (2006) 259-266.

[10] E. P. Wigner and L. Eisenbud: Higher Angular Momenta and Long Range Interaction in Resonance Reactions. Phys. Rev. 72 (1947) 29 .

[11] P. N. Racec, E. R. Racec, and H. Neidhardt: Evanescent channels and scattering in cylindrical nanowire heterostructures. Phys. Rev. B 79 (2009)155305 .

[12] V. Pagneux, N.Amir and J. Kergomard: A study of wave propagation in varying cross-section waveguides by modal decomposition. Part I: Theory and validation, J. Acoust. Soc. Am., 100 (1996) 2034-2048 .

[13] W. P. Bi, V. Pagneux, D. Lafarge, and Y. Aurégan: Modelling of sound propagation in a non-uniform lined duct using a multi-modal propagation method. J. Sound and Vib.,289 (2006) 1091-1111.

[14] H.-J. Stokmann, E. Persson, Y.-H. Kim, M. Barth, U. Kuhl, and I. Rotter: Effective hamiltonian for a microwave billiard with attached waveguide. Physical Review E 65 (2002).

[15] L. N. Trefethen: Spectral Methods in MATLAB. Society for Industrial and Applied Mathematics, Jan. 2000.